remote sensing

MDPI

Article

Prediction of Plant Diversity Using Multi-Seasonal Remotely Sensed and Geodiversity Data in a Mountainous Area

Soroor Rahmanian [1], Vahid Nasiri [2], Atiyeh Amindin [3], Sahar Karami [4], Sedigheh Maleki [5,6], Soheila Pouyan [3] and Stelian Alexandru Borz [1,*]

[1] Department of Forest Engineering, Forest Management Planning and Terrestrial Measurements, Faculty of Silviculture and Forest Engineering, Transilvania University of Brasov, 500123 Brasov, Romania
[2] Faculty of Civil Engineering, Transilvania University of Brasov, 900152 Brasov, Romania
[3] Department of Natural Resources and Environmental Engineering, College of Agriculture, Shiraz University, Shiraz 71348-14336, Iran
[4] Quantitative Plant Ecology and Biodiversity Research Lab, Department of Biology, Faculty of Science, Ferdowsi University of Mashhad, Mashhad 91779-48974, Iran
[5] Department of Plant Production, Faculty of Agriculture, University of Torbat Heydarieh, Torbat Heydarieh 95161-68595, Iran
[6] Saffron Institute, University of Torbat Heydarieh, Torbat Heydarieh 95161-68595, Iran
* Correspondence: stelian.borz@unitbv.ro; Tel.: +40-742-042-455

Abstract: Plant diversity measurement and monitoring are required for reversing biodiversity loss and ensuring sustainable management. Traditional methods have been using in situ measurements to build multivariate models connecting environmental factors to species diversity. Developments in remotely sensed datasets, processing techniques, and machine learning models provide new opportunities for assessing relevant environmental parameters and estimating species diversity. In this study, geodiversity variables containing the topographic and soil variables and multi-seasonal remote-sensing-based features were used to estimate plant diversity in a rangeland from southwest Iran. Shannon's and Simpson's indices, species richness, and vegetation cover were used to measure plant diversity and attributes in 96 plots. A random forest model was implemented to predict and map diversity indices, richness, and vegetation cover using 32 remotely sensed and 21 geodiversity variables. Additionally, the linear regression and Spearman's correlation coefficient were used to assess the relationship between the spectral diversity, expressed as the coefficient of variation in vegetation indices, and species diversity metrics. The results indicated that the synergistic use of geodiversity and multi-seasonal remotely sensed features provide the highest accuracy for Shannon, Simpson, species richness, and vegetation cover indices (R^2 up to 0.57), as compared to a single model for each date (February, April, and July). Furthermore, the strongest relationship between species diversity and the coefficient of variation in vegetation indices was based on the remotely-sensed data of April. The approach of multi-model evaluations using the full geodiversity and remotely sensed variables could be a useful method for biodiversity monitoring.

Keywords: geodiversity; remote sensing; multispectral; random forest; time series; plant diversity

Citation: Rahmanian, S.; Nasiri, V.; Amindin, A.; Karami, S.; Maleki, S.; Pouyan, S.; Borz, S.A. Prediction of Plant Diversity Using Multi-Seasonal Remotely Sensed and Geodiversity Data in a Mountainous Area. *Remote Sens.* **2023**, *15*, 387. https://doi.org/10.3390/rs15020387

Academic Editor: Michele Innangi

Received: 17 November 2022
Revised: 29 December 2022
Accepted: 6 January 2023
Published: 8 January 2023

1. Introduction

Assessing biodiversity over large geographical areas is a difficult task [1,2]. There are several traditional in situ approaches for biodiversity surveying [2–4]. In this regard, diversity indices, such as the richness, Shannon–Wiener, and Simpson indexes, including the number of individuals within plant communities, may be used to quantify taxonomic diversity [3,4]. Despite the fact that field-based botanical surveys can accurately estimate plant diversity and species composition, they are time consuming and costly, and they often lack a complete spatial coverage [5,6]. As a result, they cannot support checking for trends in biodiversity at large scales. Remote sensing can provide a wider view on the

Earth's surface across space and time [5–7] and, as a result, it has frequently been described as a promising solution to monitor biodiversity [8,9] by stepping up monitoring processes at various spatial and temporal scales. When remote sensing data are coupled with field surveys, it can lead to significant improvements and understanding of the natural world. In particular, remotely sensed imagery has become available as open data and significantly improved monitoring of the natural habitats, which is required for biodiversity conservation [10,11].

Recently, remotely sensed data have revolutionized scaled plant monitoring and has been confirmed as a useful method for mapping and monitoring biodiversity [12,13]. In contrast to other land cover types, such as forests or croplands, grasslands have not received much attention in the remote sensing literature [14]. In recent decades, the availability of satellite-based vegetation indices has increased significantly, easing the study of all parts of the world by removing the barriers brought by accessibility and time [15,16]. Spectral diversity, which is the variability in remotely sensed data, as reflected by plants, is the most important indirect observation approach, providing a broad range of possibilities for monitoring species diversity. Remotely sensed features, such as the vegetation indices, have been proved to be useful estimates of productivity and plant diversity, since they characterize vegetation attributes [16,17]; they can be used to estimate species counts or other biodiversity-related metrics from remote sensing data, and quantify the spatial non-uniformity that indicate the patterns in biodiversity [18–21]. This is based on the link between plant biodiversity and spectral variation [18,22], according to which, the variability in remotely sensed spectral patterns is connected to plant diversity [23]. Accordingly, when the plant species diversity of a specific region increases, a heterogeneous plant community is, therefore, expected to have increased spectral diversity and variability [24].

There have been many documented efforts to monitor biodiversity by remote sensing [25–27], but most of these studies have overlooked the impact of temporal dynamics in plant communities (i.e., phenology) on the remote sensing of plant diversity. Specifically, remote sensing in biodiversity studies has often been confined to data gathered at a single time [28–30], which is usually constrained by the availability of in situ data. The lack of focus on the temporal dimension was mainly caused by the difficulty of implementing repetitive field data collection campaigns, which are time consuming and costly [31].

Habitat heterogeneity, defined as the spatial and temporal variability in environmental parameters (e.g., rainfall and temperature), management processes (e.g., grazing, fire, and mowing), and other successional shifts, have been identified as fundamental ecosystem attributes affecting the patterns of biodiversity across spatial and temporal scales [32]. We presume that by providing multi-temporal data at fine spatial resolution and across large geographical extents, remote sensing can be useful in estimating environmental heterogeneity and thereby biodiversity. In this research, geodiversity and remotely sensed data were used to identify how biodiversity of grasslands changes over time. The following objectives were set to reach the goal of the study: (i) to evaluate the capability of remotely sensed features, environmental data (hereafter geodiversity), and their integration to estimate plant diversity, (ii) to identify the best time point of the year for estimating plant diversity for the study area, and (iii) to test the relationship between spectral and species diversity as a prerequisite to monitor species diversity. To do so, remotely sensed data, geodiversity features, and in situ measurements taken during the growing season in the southwest of Iran were integrated to develop machine learning algorithms for biodiversity modeling and prediction.

2. Materials and Methods

2.1. Study Area and Sampling Design

Dakal-kooh is a mountainous rangeland, which was used as the study area in this research; it covers 1756 ha, and is located in the north-west of Fars Province, Iran (51.30° to 55.57°E, and 33.32° to 33.37°N; Figure 1). The elevation of the area ranges from 920 to 1391 m (Figure 1). According to the de Martonne aridity index, the climate is semi-arid [33].

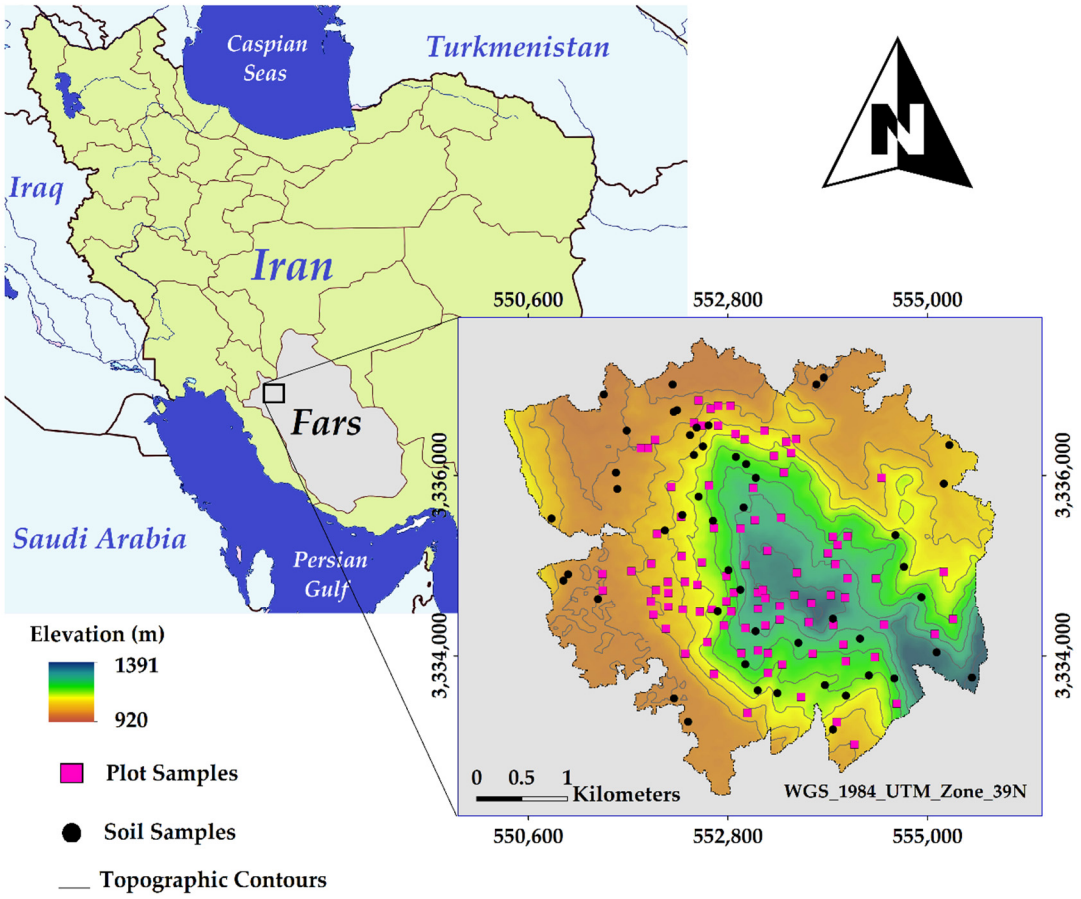

Figure 1. Geographic location of the study area used to collect species occurrence. Upper left panel—map of Iran showing the Fars province and the study area; lower right panel—study area showing the soil and vegetation plot samples.

The 11-year average rainfall is 489 mm, and the average temperature is 21 °C [33]. A total of 96 (10 × 10 m, Figure 1) plots were chosen at random throughout the study area. Each plot was spatially characterized by its geographical coordinates. In these plots, abundance (cover percentage) of all plant species was recorded between April and May of 2020. The flora in the study region is mostly made of ephemeral and perennial forbs and grasses [33]. The most common species are *Aegilops umbellulata* Zhuk, *Heteranthelium piliferum* Hochst. ex Jaub., and Spach and *Stipa capensis* Thumb, which are accompanied by *Amygdalus eburnea* Spach, *Amygdalus scoparia* Spach., *Astragalus baba-alliar* Parsa, and *Cerasus microcarpa* Boiss [33].

2.2. Data Preparation

2.2.1. Remotely Sensed Variables

Expert knowledge of vegetation, edaphic, and hydrologic characteristics were used to select a multi-seasonal collection of remotely sensed features. In this regard, the Google Earth Engine (GEE) cloud computing platform was used to create multi-seasonal Sentinel-2 (S2) and Landsat-8 (L8) surface reflectance image collections. For image collection, three-time milestones were considered: mid-winter (February 2019), when some herbaceous plant species start their growth; mid-spring (April 2020) during the peak growing season; and mid-summer (July 2020) during the senescence of most herbaceous plants (Figure 2). S2 monthly image collections were used to extract the mean spectral indices, and L8 datasets were used to extract the monthly land surface temperature (LST). These processes resulted in 32 features extracted from remotely sensed data (Table 1).

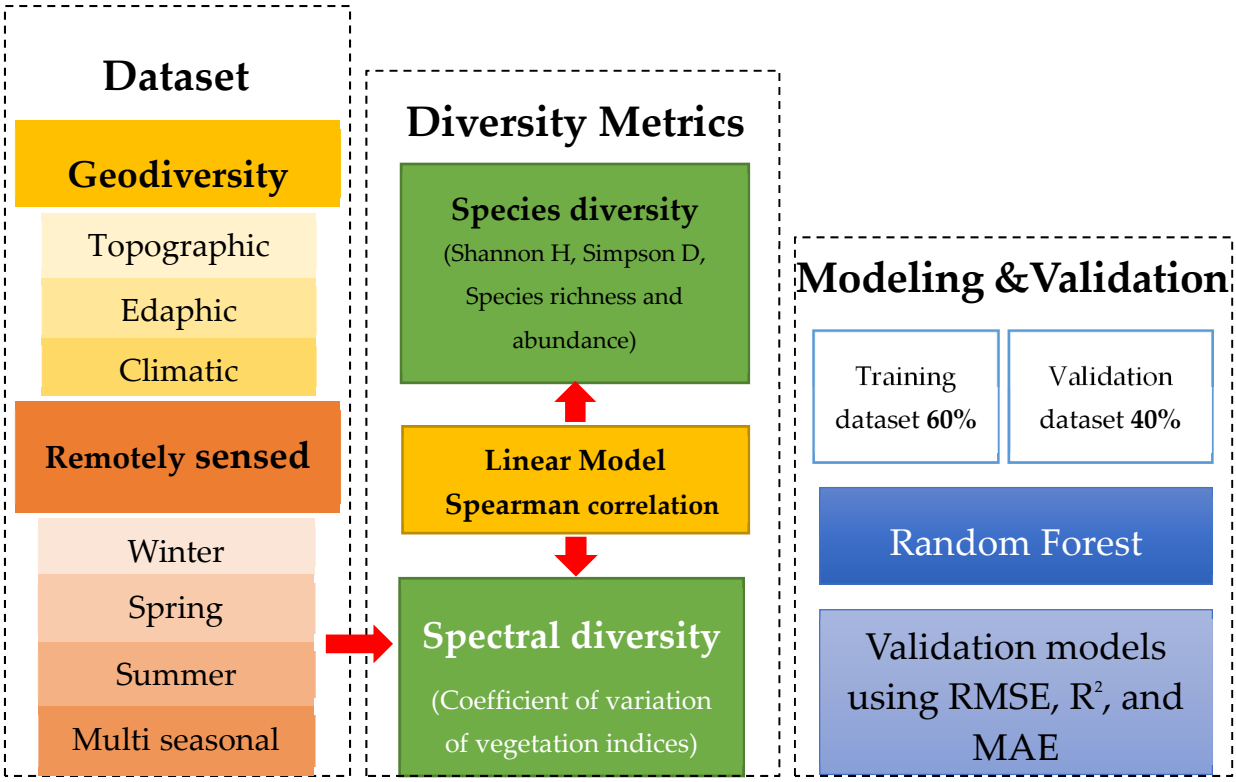

Figure 2. Datasets, metrics, and methodological steps used in this study.

Table 1. List of the spectral and geodiversity indices used in this study.

Sentinel-2 Features	Formulae	Reference
Canopy Response Salinity Index (CRSI)	$\sqrt{((B8A) \times B4 - B3 \times B2)/(B8A \times B4 + B3 \times B2)}$	[34]
Enhanced Vegetation Index (EVI)	$2.5 \times (B8A - B4)/((B8A + 6 \times B4 - 7.5 \times B2 + 1))$	[35]
Green-Red Vegetation Index (GRVI)	B3 − B4/B3 + B4	[21]
Green Normalized Difference Vegetation Index (GNDVI)	B8 − B3/B8 + B3	[36]
Normalized Difference Vegetation Index (NDVI)	B8 − B4/B8 + B4	[37]
Normalized Difference Vegetation Index red-edge 2 (NDVIre2)	B8A − B6/B8A + B6	[35]
Normalized Difference red-edge 1 (NDre1)	B8 − B5/B8 + B5	[35]
Normalized Multiband Drought Index (NMDI)	(B8A − B11 − B12)/(B8A + B11 + B12)	[35]
Normalized Difference Water Index (NDWI)	B8A − B11/B8A + B11	[38]
Soil-Adjusted Total Vegetation Index (SATVI)	$((B11 - B4))/((B11 + B4 + L)) \times (1 + L) - B12/2$	[39]
Modified Soil Adjusted Vegetation Index (MASVI)	$2B8 + 1 - \sqrt{(((B8 + 1)\hat{}2 - 8(B8 - B4))/2)}$	[40]
Normalized Shortwave-infrared Difference SM Index 3 (NSDSI3)	B11 − B12/B11 + B12	[41]
Triangular Chlorophyll Index red-edge 1 (TCIrel)	$1.2 \times (B5 - B3) - 1.5 \times (B4 - B3) \times \sqrt{(B5/B4)}$	[35]
Transformed Vegetation Index (TVI)	((B8 − B4/B8 + B4) + 0.5)0.5 × 100	[21]
Vegetation (V)	B8/B4	[42]
Brightness Index (BI)	$x = \sqrt{([\![B4]\!]\hat{}2 + [\![[\![B3]\!]\hat{}2 + B2]\!]\hat{}2)/3}$	[43]
Carbonate index (CaI)	B4/B3	[44]
Calcareous Sedimentary rocks index (CalcI)	B11 − B3/B11 + B3	[45]
Coloration index (CI)	B4 − B3/B4 + B3	[43]
Ferrous iron (FeI)	B4/B11	[44]
Geological response index (GeoI)	B11 − B12/B11 + B12	[45]
Grain size index (GSI)	(B4 − B2)/(B4 + B3 + B2)	[46]
Hue Index (HI)	(2 × B4 − B3 − B2)/(B3 − B2)	[43]
Intensity index 1 (Int1)	B3 + B4/2	[47]
Intensity index 2 (Int2)	B3 + B4 + B8A/2	[35]

Table 1. *Cont.*

Sentinel-2 Features	Formulae	Reference
Moisture Stress Index (MSI)	B11/B8	[48]
Salinity Index (S3)	B3×B4/B2	[49]
Saturation Index-T (SI-T)	B4 − B2/B4 + B2	[43]
Second Brightness Index (BI2)	$\sqrt{((B4 \times B4) + (B3 \times B3) + (B8 \times B8)/3)}$	[50]
Soil Moisture Monitoring Index (SMMI)	$\sqrt{(\lceil B8A \rceil \hat{} 2 + B\lceil 11 \rceil \hat{} 2)} / \sqrt{2}$	[35]
Visible and Shortwave Drought Index (VSDI)	1 − (B12, B4 − 2×B2)	[35]
Landsat-8 Features	**Formulas**	**Reference**
Land Surface Temperature (LST)	-	[51]
Geodiversity variables		
Altitude (ALT)	Elevation above sea level	[52]
Slope degree (SLP)	Gradient of the slope steepness	[53]
Aspect	Direction of the line of the steepest descent (r = width/height)	[53]
Plan curvature (PLC)	Rate of change of aspect along a contour	[53]
Profile curvature (PRC)	Rate of change of slope down a slope line	[53]
Stream power index (SPI)	A measure of the topographic control on the sediment transport (USLE's LS factor)	[54]
Multiresolution Index of the Ridge Top Flatnes (MRRTF)	Measure of flatness and lowness	[53]
Topographic position index (TPI)	Difference between a cell elevation value and the average elevation of the neighborhood around that cell	[55]
Topographic Ruggedness Index (TRI)	The amount of elevation difference between adjacent cells of a digital elevation model	[56]
Ultiresolution index of valley bottom flatness (MRVBF)	Measure of flatness and lowness	[53]
Mass Balance Index (MBI)	Balance between soil mass deposited and eroded	[51]
Mean annual rainfall (Rain)	The monthly average rainfall	
pH	Potential of hydrogen: scale used to specify the acidity or basicity of an aqueous solution.	
Electrical conductivity (EC)	The total of soil anions and cations	
Sand percentage (Sand)	Share of sand in the soil particle size distribution	
Clay percentage (Clay)	Share of clay in the soil particle size distribution	-
Silt percentage (Silt)	Share of silt in the soil particle size distribution	-
Soil organic carbon content (OC)	Decayed plant residues and microorganisms	
Soil organic matter content (OM)	Detritus of plant and animal, soil microbes, and substances that soil microbes synthesize at various stages of decomposition.	
Soil Nitrogen content (N)	Both organic and inorganic forms of Nitrogen in the soil	

2.2.2. Geodiversity Variables

Geodiversity variables used in this study were a combination of topographic, climatic, and edaphic variables (Figure 2). Twelve topographic factors were considered, namely the altitude (ALT), slope degree (SLP), aspect (ASP), profile (PRC) and plan curvatures (PLC), stream power index (SPI), Multiresolution Index of the Ridge Top Flatness (MRRTF), topographic position index (TPI), topographic wetness index (TWI), Topographic Ruggedness Index (TRI), multiresolution index of valley bottom flatness (MRVBF), and Mass Balance Index (MBI). The freely available ALOS PALSAR—Radiometric Terrain Correction DEM (https://vertex.daac.asf.alaska.edu/ accessed on 16 November 2022), with a resolution of 12.5 m, was used to generate the topographic layers.

Long-term mean annual rainfall (Rain), calculated based on the datasets provided by the Meteorological Office of Fars province (http://www.farsmet.ir accessed on 16 November 2022), was used as a climatic variable. Moreover, soil acidity (pH), electrical conductivity (EC), sand, clay, and silt percentages, organic carbon (OC) content, organic matter content (OM), and nitrogen content (N) were used to specify the edaphic features. In this regard, 50 samples were collected in the upper layer (0 to 30 cm in depth) of the soils from the

study area during the study of Rahmanian et al. [2]. These were used herein to evaluate the relevant soil parameters across the study area (Figure 1). Procedures used to process the soil samples and to estimate the relevant properties are given in Rahmanian et al. [2]. Then, the edaphic values were interpolated using the inverse distance weighting (IDW) interpolation method to generate raster layers. In IDW interpolation, the closest measured values place more weight on determining the anticipated value than those further away [57]. IDW was performed by using the ArcGIS geoprocessing tool (version 10.8).

2.3. Statistical Analysis

2.3.1. Statistical Workflow

This study considered the available geodiversity and time series of remotely sensed variables that can predict the plant diversity metrics in the study area. To find the most important variables that affect plant diversity, a multicollinearity analysis was used. To characterize plant diversity, in addition to the species richness and vegetation cover that were recorded during field sampling in each plot, the most popular diversity metrics, such as the Simpson (sensitive-to-dominant species) and Shannon (sensitive-to-rare species) indices, were estimated for each plot. To map and predict species diversity (Shannon's, Simpson's indexes), and species richness and vegetation cover, several random forest (RF) models were developed based on the set of remotely sensed and geodiversity variables, as well as based on a combination of them in three seasons (winter, spring, and summer). To find out which variables placed the most importance on predicting plant diversity and vegetation attributes, a variable importance analysis was implemented. In addition, spectral diversity is characterized hereafter by the coefficient of variation (CV), which reflects the variation in remote sensing data spectrum based on the patterns in vegetation characteristics of the plant species. Since CVs of vegetation indices are related to traditional measures of plant diversity [58], the relationships between CVs of vegetation indices, species diversity, and vegetation cover were tested to estimate plant diversity.

2.3.2. Preparation of Variables

By multicollinearity testing of independent variables, only the most influential variables were kept among the associated pairs using a stepwise process. The strongly associated variables were excluded to avoid potential overfitting issues. The "vifstep" function of "usdm" R package was used to examine the collinearity among the 53 variables used in this study. The variance inflation factor (VIF) and tolerance (T) were used as metrics in multicollinearity testing. The presence of significant collinearity was defined for the condition in which the VIF index was larger than 5.0 and T was less than 0.1 [59]. By locating and eliminating strongly associated variables, the size of the datasets was reduced (Table 2).

Diversity metrics, namely species richness, Shannon and Simpson indices, and also vegetation cover, were measured in this study. Species richness stands for the number of species for which ground sampling makes it easier to obtain an accurate value. Percentage cover is an abundance measurement metric that indicates how much space a species occupies in a plot, and it was recorded during the field sampling. R software (version 3.5.1) was used to calculate Shannon's H and Simpson's D diversity indices by implementing the package "vegan" (R Core Team, R Foundation for Statistical Computing, Vienna, Austria). These two indices take species uniformity into account and were calculated using the following equations [60,61]:

$$\text{Shannons Index (H)} = -\sum[p_i \times \ln(p_i)] \quad (1)$$

$$\text{Simpsons Index (D)} = 1/\sum(p_i)^2 \quad (2)$$

where p_i is the ratio (n/N) of the number of individuals of one species (n) to the total number of individuals (N). The number of species present in an environment is described as the species richness [62].

Table 2. Results of general linear models testing the effects of geodiversity and spectral variables on plant species diversity (Shannon H and Simpson), richness, and vegetation cover in the selected seasons.

	Shannon									**Simpson**								
	February			**April**			**July**			**February**			**April**			**July**		
	R	R^2	*p* value	R	R^2	*p* value	R	R^2	*p* value	R	R^2	*p* value	R	R^2	*p* value	R	R^2	*p* value
GNDVI	0.15	0.02	0.08	0.27	0.11	**0.002**	0.15	0.03	0.058	0.06	0.01	0.13	0.26	0.08	0.005	0.13	0.01	0.15
GRVI	0.13	0.01	0.13	0.28	0.07	**0.01**	0.14	0.025	0.09	0.18	0.03	0.06	0.25	0.05	0.025	0.21	0.05	**0.02**
MASVI	0.32	0.08	**0.006**	0.48	0.18	**<0.001**	0.24	0.08	0.007	0.34	0.13	**0.001**	0.47	0.16	<0.001	0.37	0.14	**<0.001**
Ndre1	0.15	0.02	0.09	0.36	0.15	**<0.001**	0.20	0.046	0.035	0.08	0.02	0.11	0.36	0.13	<0.001	0.16	0.02	0.116
NDVIre2	0.16	0.02	0.09	0.35	0.15	**<0.001**	0.19	0.045	0.03	0.1	0.02	0.09	0.35	0.13	<0.001	0.16	0.01	0.126
SATVI	0.24	0.06	**0.01**	0.44	0.17	**<0.001**	0.24	0.084	0.006	0.32	0.15	**0.002**	0.47	0.18	<0.001	0.37	0.15	**<0.001**
NDVI	0.07	0.006	0.46	0.28	0.06	**0.02**	0.19	0.04	0.047	0.28	0.08	**0.008**	0.35	0.11	0.002	0.23	0.03	**0.051**
TCIre1	0.12	0.002	0.37	0.34	0.13	**<0.001**	0.17	0.007	0.21	0.14	0.01	0.15	0.38	0.14	<0.001	0.11	0.008	0.21
VSDI	0.14	0.01	0.12	0.33	0.13	**<0.001**	0.18	0.016	0.14	0.12	0.04	**0.04**	0.33	0.12	0.001	0.14	0.01	0.17
V	0.07	0.006	0.46	0.28	0.06	**0.02**	0.12	0.016	0.14	0.28	0.08	**0.008**	0.35	0.11	0.002	0.16	0.01	0.16
TVI	0.19	0.04	**0.03**	0.34	0.13	**<0.001**	0.13	0.007	0.512	0.13	0.03	**0.07**	0.37	0.14	<0.001	0.08	−0.01	0.72
EVI	0.006	−0.01	0.78	0.19	0.02	**0.09**	0.12	0.012	0.168	0.25	0.07	**0.01**	0.32	0.08	0.005	0.20	0.03	**0.05**
CRSI	0.40	0.16	**0.001**	0.49	0.19	**<0.001**	0.05	0.013	0.80	0.32	0.14	**0.001**	0.41	0.14	<0.001	0.13	−0.01	0.83
	Richness									**Vegetation cover**								
	February			**April**			**July**			**February**			**April**			**July**		
	R	R^2	*p* value	R	R^2	*p* value	R	R^2	*p* value	R	R^2	*p* value	R	R^2	*p* value	R	R^2	*p* value
GNDVI	0.06	0.001	0.34	0.10	0.02	0.13	0.10	0.006	0.23	0.005	0.01	0.64	0.04	0.003	0.39	0.01	0.03	0.87
GRVI	0.22	0.049	**0.03**	0.33	0.12	**0.001**	0.37	0.14	**<0.001**	0.11	0.07	0.2	0.16	0.04	**0.03**	0.08	0.005	0.44
MASVI	0.22	0.03	0.06	0.27	0.06	**0.01**	0.29	0.09	**0.005**	0.06	0.01	0.61	0.06	0.004	0.41	0.05	0.008	0.52
Ndre1	0.10	0.005	0.24	0.22	0.06	**0.01**	0.16	0.023	0.10	0.05	0.01	0.4	0.09	0.001	0.29	0.06	0.008	0.52
NDVIre2	0.11	0.005	0.23	0.21	0.06	**0.01**	0.17	0.025	0.09	0.04	0.01	0.41	0.09	0.002	0.27	0.07	0.007	0.49

Table 2. *Cont.*

	Richness									Vegetation cover								
	February			April			July			February			April			July		
	R	R^2	*p* value	R	R^2	*p* value	R	R^2	*p* value	R	R^2	*p* value	R	R^2	*p* value	R	R^2	*p* value
SATVI	0.20	0.03	0.06	0.25	0.05	**0.02**	0.26	0.08	**0.008**	0.09	0.03	0.51	0.06	0.005	0.43	0.05	0.007	0.51
NDVI	0.15	0.02	0.09	0.21	0.06	0.14	0.17	0.03	0.06	0.11	0.04	0.93	0.04	0.007	0.21	0.06	0.013	0.97
TCIre1	0.12	0.002	0.36	0.22	0.07	**0.01**	0.05	0.009	0.57	0.04	0.01	0.5	0.07	0.001	0.35	0.03	0.009	0.57
VSDI	0.09	0.005	0.23	0.20	0.06	**0.02**	0.18	0.016	0.14	0.04	0.02	0.42	0.10	0.005	0.24	0.09	0.003	0.38
V	0.15	0.02	0.09	0.22	0.07	**0.01**	0.08	0.002	0.27	0.01	0.01	0.93	0.04	0.006	0.22	0.14	0.008	0.52
TVI	0.13	0.004	0.25	0.21	0.05	**0.03**	0.02	0.013	0.95	0.01	0.01	0.65	0.03	0.008	0.54	0.22	0.03	0.07
EVI	0.11	0.003	0.27	0.15	0.02	0.11	0.12	0.005	0.30	0.13	0.07	0.51	0.01	0.01	0.62	0.09	0.007	0.50
CRSI	0.21	0.03	0.06	0.24	0.05	**0.03**	0.26	0.019	0.12	0.06	0.01	0.59	0.06	0.004	0.42	0.18	0.005	0.33

To monitor spectral diversity, which refers to the variation in remote sensing measurements, the vegetation indices (GNDVI, GRVI, MASVI, Ndre1, NDVIre2, SATVI, TCIre1, VSDI, V, TVI, EVI, MSAVI, and CRSI) were used as input for estimating the coefficient of variation (CV) between all the pixels inside the study area. The CV was calculated across the entire study area as the standard deviation divided by the mean value of all pixels located in a reference moving window of 3 × 3 pixels [63,64]. Then, the pixel values were extracted for the 96 studied plots as these pixel values relate to conventional metrics of biodiversity [63].

The linear regression and Spearman's correlation coefficient were used to find out what kind of relationship exists between CV of vegetation indices and plant diversity metrics (Shannon, Simpson, richness, and vegetation cover). By this approach, the aim was to find if there was a strong relationship, and which relationship was the strongest between the coefficient of variation in vegetation indices and diversity metrics.

2.4. Modeling Species Diversity by Random Forest

Several random forest (RF) machine learning models were used to map and predict species diversity (Shannon's, Simpson's, and richness indexes) and vegetation cover, taking the remotely sensed, topographic, climatic, and edaphic variables as inputs. A training sample accounting for 60% of the plots was used. RF is a machine learning algorithm that consists of an ensemble of bootstrapped trees, which are used to reach a vote-based decision, making it useful and performant in classification and regression problems [65]. RF generates accurate forecasts that are simple to comprehend, and it is able to effectively handle large datasets. Compared to the decision tree algorithm, RF is more accurate in forecasting outcomes [66,67].

In total, 48 models were developed to predict four plant diversity indices (Shannon, Simpson, richness and vegetation cover) by considering four time milestones (February, April and July, and their aggregate expressed as multi-seasonal) and three groups of variables (geodiversity, remotely sensed, and a combination of the two). In detail, a subset of sixteen RF models were based on the remotely sensed data and were developed for each of the plant diversity indices (Shannon and Simpson), species richness, and vegetation cover; of these, three models were developed to predict plant diversity for each time milestone (February, April, and July), with remotely sensed variables (Table A1, Appendix A), and one model was used to predict plant diversity for all time milestones (multi-seasonal) considered together (Table A1, Appendix A). Moreover, a subset of sixteen RF models were developed taking the geodiversity variables as inputs (Table A1, Appendix A) to predict diversity indices (Shannon and Simpson), richness and vegetation cover for each time milestone, and one model using geodiversity variables was developed to predict plant diversity for all time milestones considered together (Table A1, Appendix A). Finally, twelve models were developed using the final set of remotely sensed and geodiversity variables (Table A1, Appendix A) for each time milestone (February, April, and July), and one model was developed for all the time milestones (multi-seasonal), with a combination of all geodiversity and remotely sensed variables (Table A1, Appendix A). Then, the maps of diversity metrics were prepared based on the final set of remotely sensed and geodiversity variables.

To understand the importance of geodiversity and remotely sensed variables in predicting plant diversity metrics of each time milestone (February, April, and July) by RF models, variable importance measure was estimated [65,68] in "Caret" package of R [69]. Ten of the most important variables were selected based on their scores, which were scaled from 0 to 100 [70].

RF models were developed in "randomForest" R package, and two main hyperparameters related to this model were tuned to enhance the modelling performance in terms of learning and generalization: the number of random variables used in each tree (mtry) and the number of regression trees (ntree), which was optimized based on an out-of-bag estimate error [65]. To infer the optimal values of these hyperparameters, a ten-fold cross-

validation resampling with 50 iterations was applied to the training samples. For more details about the optimal values of hyperparameters, see Table 3.

Table 3. Accuracy assessment results of single-date and multi-seasonal RF models based on each of the geodiversity- or remotely sensed-only variables and their hyperparameter data.

Time Scale					**Multi-Seasonal**				**April**
Diversity Metrics	Variables	RMSE	R^2	MAE	Tuning Parameters	RMSE	R^2	MAE	Tuning Parameters
Richness	All	0.075	0.27	0.058	mtry = 67; ntree = 600	0.08	0.26	0.06	mtry = 2; ntree = 500
	Geodiversity	0.087	0.2	0.060	mtry = 21; ntree = 500	0.08	0.25	0.061	mtry = 2; ntree = 500
	Remotely sensed	0.091	0.20	0.062	mtry = 49; ntree = 550	0.08	0.19	0.062	mtry = 2; ntree = 500
Vegetation cover	All	0.110	0.20	0.092	mtry = 67; ntree = 550	0.112	0.17	0.085	mtry = 32; ntree = 550
	Geodiversity	0.119	0.19	0.089	mtry = 11; ntree = 600	0.112	0.17	0.086	mtry = 2; ntree = 500
	Remotely sensed	0.117	0.19	0.089	mtry = 49; ntree = 550	0.11	0.21	0.085	mtry = 2; ntree = 500
Shannon	All	0.290	0.28	0.237	mtry = 34; ntree = 500	0.312	0.28	0.239	mtry = 17; ntree = 550
	Geodiversity	0.290	0.18	0.201	mtry = 21; ntree = 500	0.338	0.26	0.27	mtry = 10; ntree = 500
	Remotely sensed	0.310	0.25	0.228	mtry = 25; ntree = 500	0.368	0.20	0.293	mtry = 2; ntree = 500
Simpson	All	0.021	0.44	0.018	mtry = 2; ntree = 500	0.023	0.43	0.019	mtry = 2; ntree = 450
	Geodiversity	0.020	0.40	0.017	mtry = 2; ntree = 500	0.024	0.39	0.018	mtry = 2; ntree = 450
	Remotely sensed	0.020	0.26	0.019	mtry = 4; ntree = 500	0.027	0.25	0.022	mtry = 2; ntree = 450
					February				July
Diversity Metrics	Variables	RMSE	R^2	MAE	Tuning parameters	RMSE	R^2	MAE	Tuning parameters
Richness	All	0.080	0.25	0.063	mtry = 32; ntree = 500	0.083	0.22	0.064	mtry = 9; ntree = 500
	Geodiversity	0.085	0.24	0.063	mtry = 10; ntree = 500	0.083	0.21	0.064	mtry = 2; ntree = 450
	Remotely sensed	0.080	0.18	0.063	mtry = 2; ntree = 500	0.089	0.22	0.069	mtry = 9; ntree = 450
Vegetation cover	All	0.118	0.17	0.093	mtry = 2; ntree = 500	0.124	0.21	0.095	mtry = 2; ntree = 500
	Geodiversity	0.124	0.17	0.098	mtry = 2; ntree = 450	0.127	0.20	0.094	mtry = 2; ntree = 500
	Remotely sensed	0.121	0.17	0.095	mtry = 2; ntree = 450	0.122	0.20	0.095	mtry = 2; ntree = 500
Shannon	All	0.330	0.27	0.248	mtry = 28; ntree = 500	0.321	0.27	0.244	mtry = 19; ntree = 500
	Geodiversity	0.309	0.30	0.241	mtry = 2; ntree = 400	0.325	0.27	0.243	mtry = 2; ntree = 500
	Remotely sensed	0.406	0.28	0.314	mtry = 2; ntree = 400	0.336	0.25	0.264	mtry = 2; ntree = 500
Simpson	All	0.023	0.42	0.018	mtry = 2; ntree = 500	0.025	0.38	0.021	mtry = 2; ntree = 500
	Geodiversity	0.023	0.53	0.017	mtry = 2; ntree = 500	0.025	0.37	0.021	mtry = 11; ntree = 500
	Remotely sensed	0.023	0.51	0.018	mtry = 2; ntree = 500	0.027	0.24	0.0226	mtry = 9; ntree = 500

Evaluation of the Models' Performance

Spatial distribution of the Shannon's, Simpson's, richness', and vegetation cover's indexes in the three studied seasons was predicted by RF (Figure 3). Based on the species presence in the sampling plots, the values of predicted diversity, vegetation cover, and richness were extracted from the maps obtained for the considered seasons. Models' performance was evaluated by using the conventional methods of comparing the predicted values against those from the testing samples (40% of plots Section 2.1). The used metrics were the root mean square error (RMSE), mean absolute error (MAE), and the coefficient of determination (R^2) [71,72].

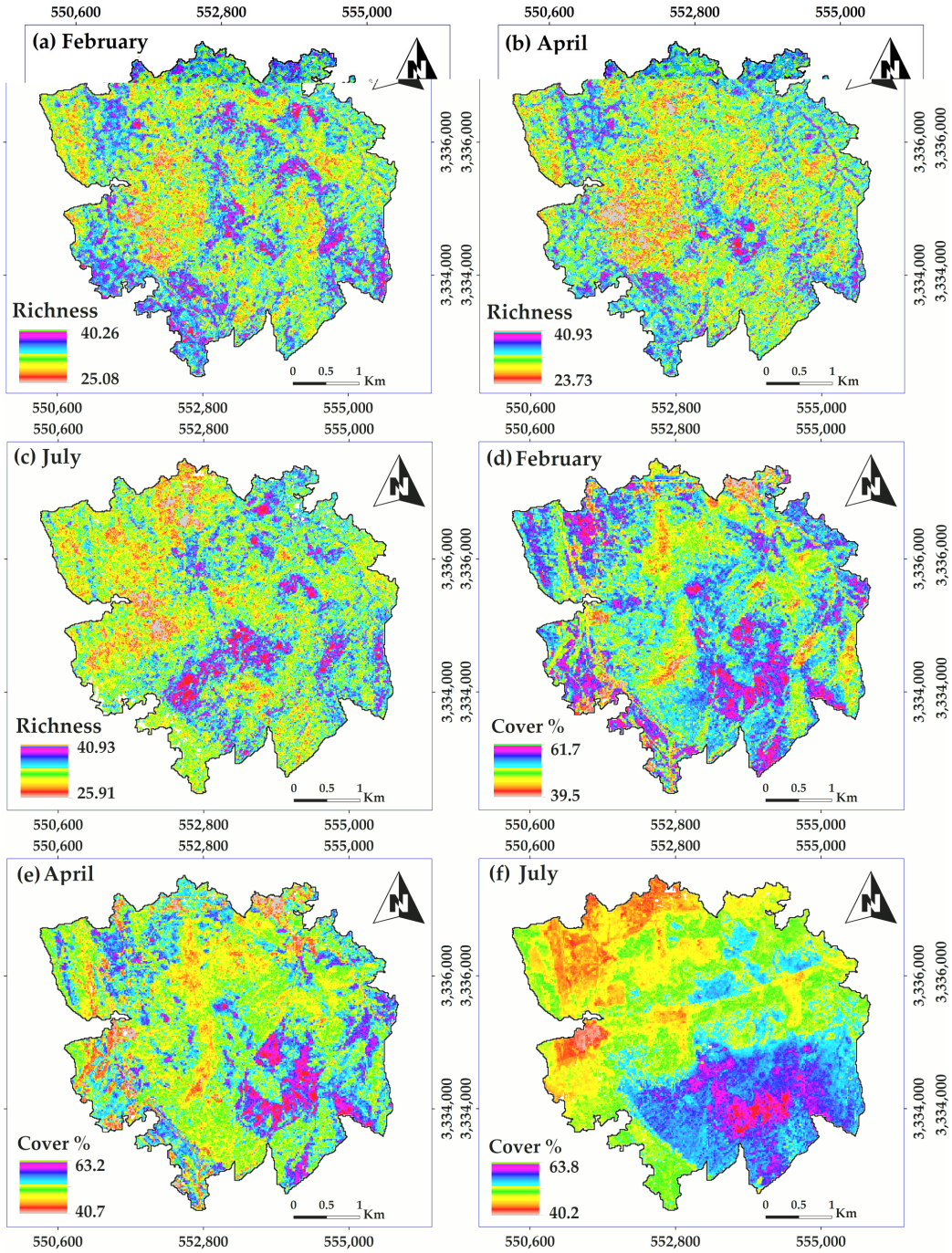

Figure 3. *Cont.*

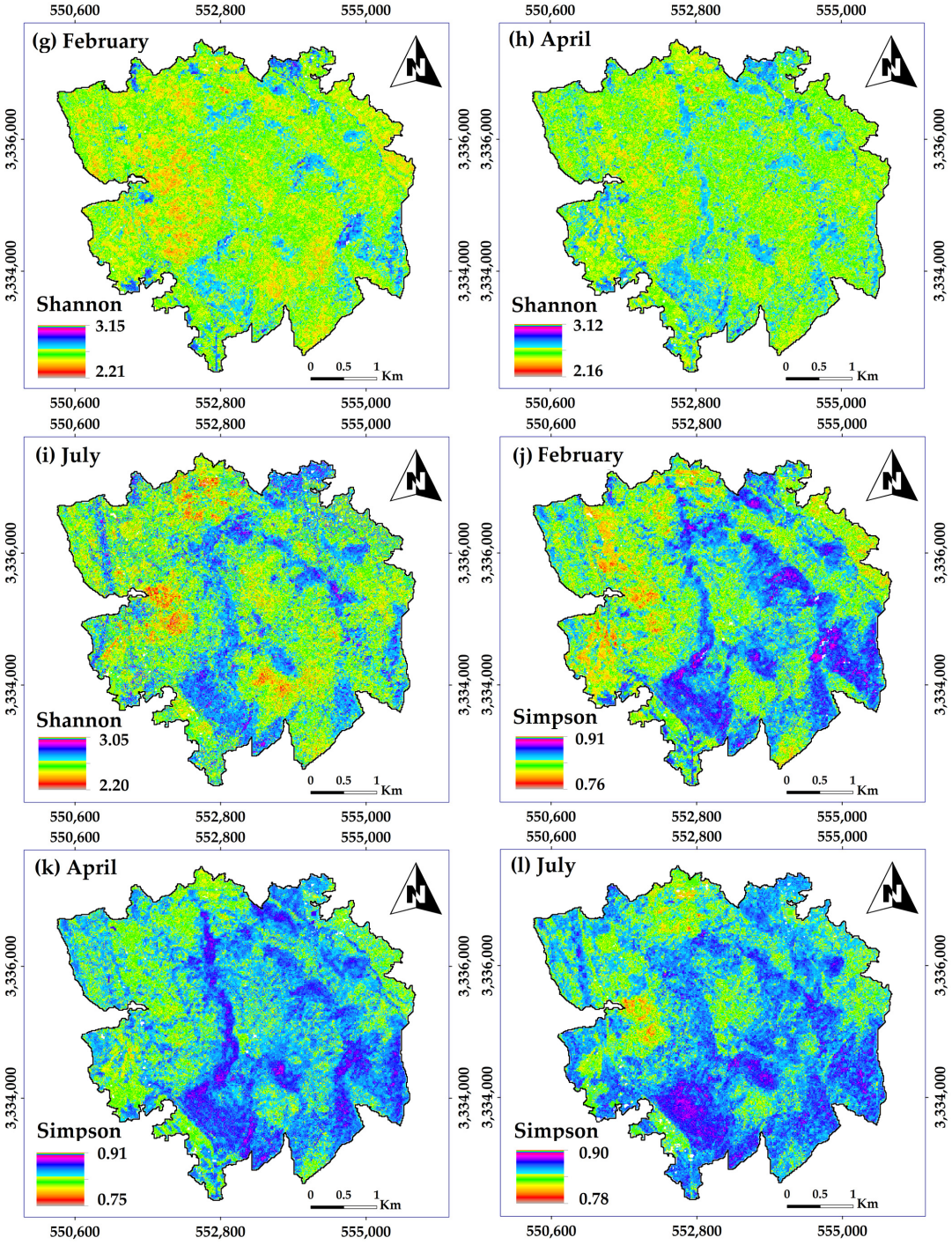

Figure 3. Spatial distribution of richness for February (**a**), April (**b**), and July (**c**); *vegetation cover* for February (**d**), April (**e**), and July (**f**); Shannon for February (**g**), April (**h**), and July (**i**); and Simpson for February (**j**), April (**k**), and July (**l**).

3. Results

3.1. Multicollinearity of Independent Variables

The multicollinearity test results showed that lithology, wind, SLP, ASP, Rain, PLC, PRC, TWI, NSDSI3, GNDVI, NDVI, SATVI, VDSI, GRVI, TVI, ClaI, GRVI, NDVIre1, Ndre1, BI, S3, SI, NMDI, Int1, Int2, and BI2 were strongly correlated with other variables for the February dataset; therefore, these variables were excluded. Wind, SLP, sand, NDSI3, GSI, SI, GRVI, OC, BI, CaI, NDVIre, NDre1, GSI, TVI, Int1, Int2, NDWI, SI, GNDVI, CalsI, CI, V,

SMMI, SAVI, MASVI, VDSI, and MSI were significantly correlated with other variables in the April dataset, and, therefore, they were excluded. For similar reasons, wind, sand, SI, NSDSI3, OC, Int1, Int2, CI, LSWI, BI, BI2, MSAVI, GNDVI, GRVI, SMMI, CalcI, NDre1, and NDWI were deleted from the July dataset. The list of variables kept for further analysis is shown in Table A1.

3.2. Relationship between Species and Spectral Diversity

The results of the general linear model analysis demonstrated a significant positive relationship ($p < 0.05$) between the CV of vegetation indexes, diversity indices, and vegetation cover in all three seasons. However, the mid-spring had the highest relationship between species diversity and the CV of vegetation indices. Among the diversity metrics, Shannon's and Simpson's indices showed a stronger relationship with spectral diversity (expressed as the CV of vegetation indices), as opposed to the species richness and vegetation cover (Table 2). These indices were correlated with most of the CV of vegetation in mid-spring (see Table 2 for more details). Furthermore, for mid-winter and mid-summer there were few significant relationships between the diversity indices and the CV of vegetation indices (Table 2). In mid-winter, TVI, MASVI, and CRSI significantly correlated with the Shannon index, and MASVI, SATVI, NDVI, VSDI, V, EVI, and CRSI had a significant correlation with the Simpson index. Moreover, only GRVI had a correlation with species richness. In mid-summer, MASVI, Ndre1, NDVIre2, SATVI and NDVI, SATVI and MASVI, GRVI, and MASVI and SATVI had significant correlations with the Shannon, Simpson, and richness indexes, respectively.

3.3. Performance of Plant Diversity Prediction and Mapping Accuracy

A summary of the models developed by using the full set of geodiversity and remotely sensed variables and testing samples is presented in Table 3. The results indicated that predictions of the examined diversity indices and species richness were more accurate when using multi-seasonal models for Shannon's (R^2 = 0.28, RMSE = 0.29, MAE = 0.237), Simpson's (R^2 = 0.44, RMSE = 0.02, MAE = 0.018), and species' richness indexes (R^2 = 0.27, RMSE = 0.075, MAE = 0.58) as well as vegetation cover (R^2 = 0.2, RMSE = 0.11, MAE = 0.092). Regarding the single date models, the best results were produced using the April combined data model; results for Shannon's (R^2 = 0.28, RMSE = 0.312, MAE = 0.239), Simpson's (R^2 = 0.43, RMSE = 0.023, MAE = 0.019), and species' richness indexes (R^2 = 0.26, RMSE = 0.08, MAE = 0.6), as well as vegetation cover (R^2 = 0.17, RMSE = 0.112, MAE = 0.085), are shown in Table 3.

The comparison of the validation results for the best-performing diversity models based on all variables, geodiversity- or remotely sensed-only variables, indicated that using the first option returned more accurate predictions in multi-seasonal and single-date models, except for vegetation cover (R^2 = 0.21; RMSE = 0.11; MAE = 0.85) in April, which was more accurately predicted by the use of remotely sensed variables, as well as Shannon's (R^2 = 0.3; RMSE = 0.3; MAE = 0.24) and Simpson's indices (R^2 = 53; RMSE = 0.023; MAE = 0.017), for February models, which were more accurately predicted by geodiversity variables. Moreover, the accuracy results obtained from all single-date and multi-seasonal models suggest that models predicting the Simpson's diversity were the best performing ones (Table 3). As the most precise models using the entire geodiversity and remotely sensed datasets, three single dates are shown in Figure 3 to depict the mapping of the best plant diversity prediction based on the RF models.

3.4. The Most Predictive Independent Variables

As shown in Figures 4–6, the results indicate the relevance of the best-selected models for species diversity, richness, and vegetation cover indicators. The findings on the variable importance analysis revealed that in mid-winter (February) and mid-summer (July), remotely sensed variables had more importance than geodiversity variables (Figures 4 and 6). In this regard, Soil Adjusted Total Vegetation Index (SATVI), Ferrous Iron (FeI), En-

hanced Vegetation Index (EVI), Saturation Index-T (SI-T), Canopy Response Salinity Index (CRSI), Carbonate Index (CaI), Normalized Difference Vegetation Index (NDVI), Normalized Difference red-edge 1 (NDre1), and Green Normalized Difference Vegetation Index (GNDVI) were the most important remotely sensed variables among the spectral variables in mid-winter for modeling and predicting the diversity (Figure 4), whereas Topographic Ruggedness Index (TRI), Mass Balance Index (MBI), and Plan Curvature (PLC) were the most important geodiversity variables (Figure 4).

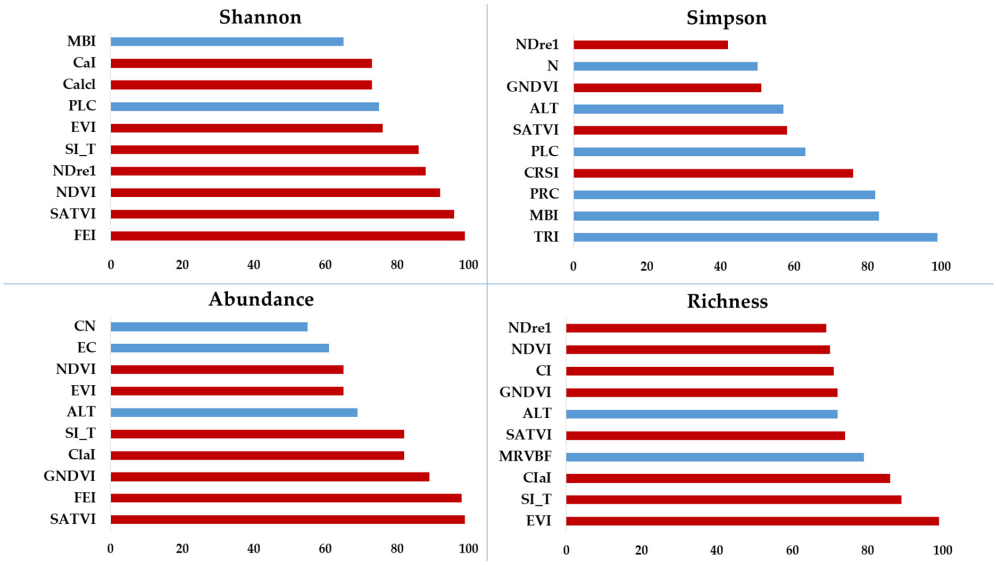

Figure 4. Ten of the most important variables in modeling and predicting the Simpson's, Shannon's, and richness' indexes, as well as vegetation cover in February for RF models, based on remotely sensed and geodiversity variables. Remotely sensed variables are shown in red, and geodiversity variables are shown in blue.

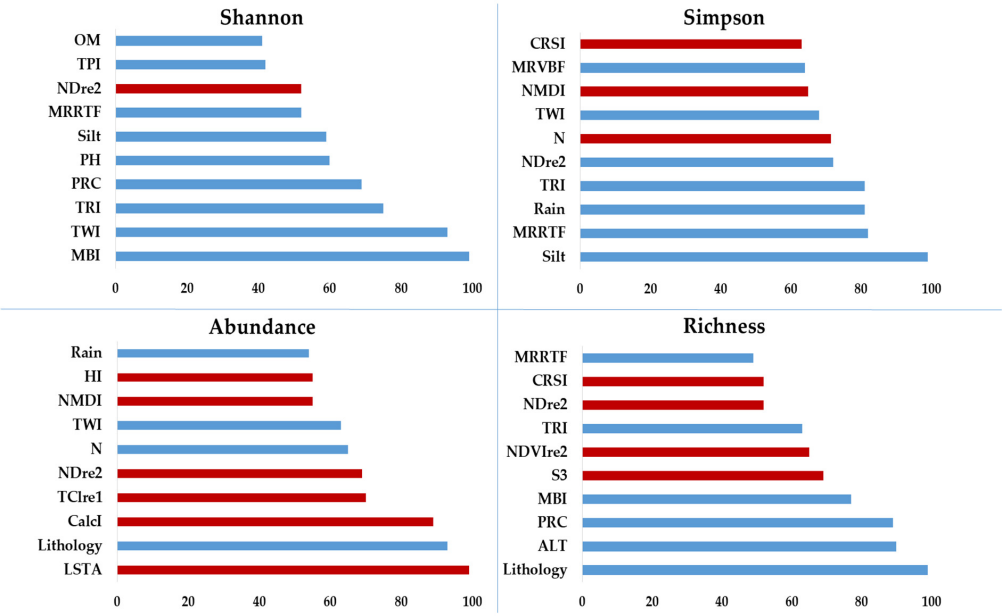

Figure 5. Ten of the most important variables in modeling and predicting the Simpson's, Shannon's, and richness' indexes, as well as vegetation cover in April for RF models, based on remotely sensed and geodiversity variables. Remotely sensed variables are shown in red, and geodiversity variables are shown in blue.

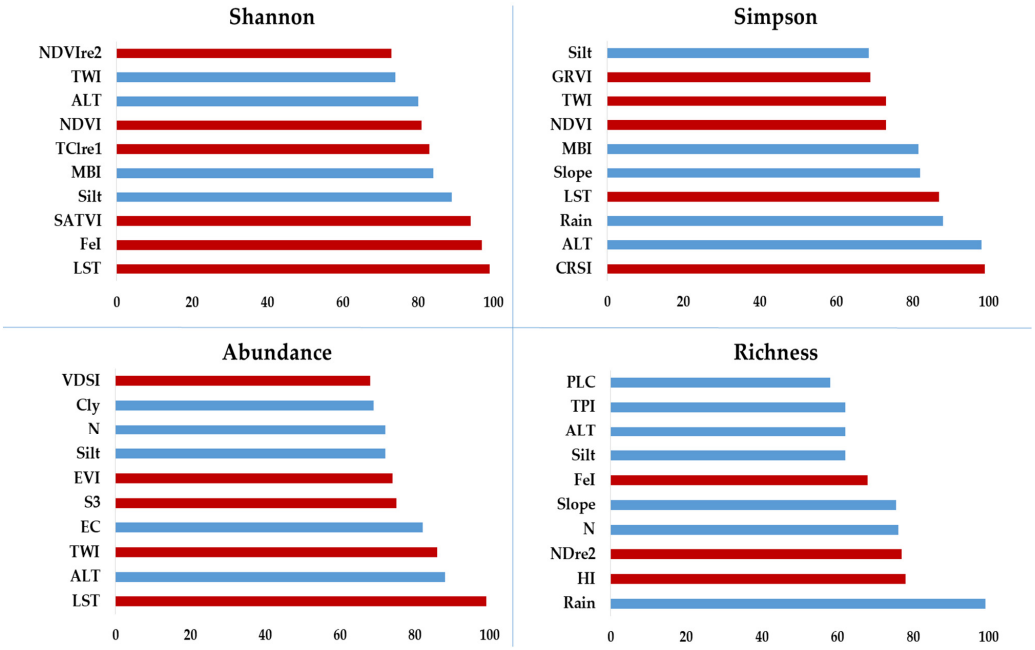

Figure 6. Ten of the most important variables in modeling and predicting the Simpson's, Shannon's, and richness' indexes, as well as vegetation cover in July for RF models, based on remotely sensed and geodiversity variables. Remotely sensed variables are shown in red, and geodiversity variables are shown in blue.

Regarding the most important variables in mid-summer (July), land surface temperature (LST), Canopy Response Salinity Index (CRSI), Hue Index (HI), Soil Adjusted Total Vegetation Index (SATVI), Normalized Difference red-edge 1 (Ndre1), and Ferrous iron (FeI) were the most important spectral variables while rainfall (Rain), altitude (ALT), Topographic Wetness Index (TWI), nitrogen content (N), electrical conductivity (EC), and slope (SLP) were the most important geodiversity variables that influenced the prediction of Shannon's, Simpson's, and richness' indexes, as well as vegetation cover (Figure 6).

In contrast, in mid-spring (April), the geodiversity variables were more important compared to the remotely sensed variables in modeling and predicting the vegetation cover, richness, and species diversity. For instance, the geodiversity variables, including Mass Balance Index (MBI), rainfall (Rain), Topographic Wetness Index (TWI), Topographic Ruggedness Index (TRI), lithology, altitude (ALT), silt, Multiresolution Index of the Ridge Top Flatness (MRRTF), and profile curvature (PRC), and remotely sensed variables, including land surface temperature (LST), Calcareous Sedimentary Rocks Index (CalcI), and Salinity Index (S3), were the important variables (Figure 5).

4. Discussion

In this study, test results for the best-performing diversity models indicated that the full set of predictor variables was more accurate than the subsets of variables taken separately (spectral- or geodiversity data) in multi-seasonal and single-date models (Table 3), which is in agreement with findings of Chrysafis et al. [73,74] and Senf et al. [75]. As for this study, the accuracy of the February, April, and July models was significantly enhanced when remotely sensed and geodiversity variables were combined. This is related to the relative importance of the input variables in each model, which leads to different contributions to model fitting. The reason is that RF is not a parsimonious method and uses all of the variables in the datasets to make predictions [76]. In addition to that, the predictions of plant diversity by the use of combined geodiversity and time series of remotely sensed data had a greater accuracy on a multi-seasonal model compared to single dates. This may be related to the fact that multi-seasonal satellite imagery captures the whole spectrum of

phenological variations in various species, boosting the spectral differentiation [74,77,78]. The effectiveness of multi-seasonal models of this study is consistent with prior research findings. For example, the combination of two remotely sensed images recorded in winter and summer periods increased forest tree diversity prediction performance in northern Greece [79].

Concerning the single dates, the prediction of species diversity was found to be more accurate on the scenes acquired in April compared to those of February and July. This may be due to the optimal vegetation and high photosynthesis of April that enabled the capturing of the vegetation changes in the reflectance of fully formed leaves. The reduced photosynthetic activity of both evergreen and deciduous plants, as well as the water deficit in the preceding months, might explain the image's low accuracy in July. Additionally, the poor accuracy in February might be because the leaf emergence did not start for many of the deciduous plants in the area. To back up these findings, a previous study has shown that the detection of species diversity is most accurate during the change over seasons (February in our instance), while spectral imaging precision is the highest during the growing season [79]. In contrast, Torresani et al. [80] found a greater link between tree species diversity and variance in reflectance as of July in south Tyrol (Italy). Additionally, Arekhi et al. [81] stated that the image taken in the summer helped to develop the most appropriate model by examining the link between various Landsat TM spectral bands (original and synthetic) and tree diversity (Shannon's index) in a temperate forest from Turkey.

Vegetation indices (VI) were found to be important parameters for monitoring plant diversity in the study area. The spectral diversity measured by the coefficient of variation in vegetation indices (CV) measures the amount of variation stored in each vegetation index, and this variability is thought to imply increased environmental heterogeneity related to diverse species composition and species diversity [82]. The results indicated a significant relationship between spectral diversity, calculated as the coefficient of variation in vegetation indices, and species diversity, calculated as Shannon's diversity index, Simpson's diversity index, species richness, and vegetation cover. The CV demonstrates that the three seasons hold separate mechanisms in controlling this variation. In comparison to winter and summer, in the spring there is a stronger relationship between the increased CV of vegetation indices and the increase in plant diversity metrics that reflects the heterogeneity of the vegetation spectrum caused by some variability in species characteristics, including phenological and physiological traits of plant species. As found in this study, remotely sensed vegetation indices help in estimating the plant diversity. This result is consistent with previous studies [83–85]. Moreover, the results of this study showed that the relationship between Shannon's and Simpson's diversity index and the CV of vegetation indices as spectral diversity were stronger than the species richness and vegetation cover. Both Simpson and Shannon diversity indices are metrics that consider the abundance of species in a given plot. However, species richness values may appear to be high due to the rare species that are present in the plots. Compared to the spectral diversity that depends on the relative abundance of each species, it has been demonstrated that Shannon and Simpson indices, which take species abundance into account, are more accurate.

Concerning the variable importance of the models used in this study, diversity indices of different seasons were not equally related to the landscape features. For instance, the most important variables affecting plant diversity metrics were topographic variables and vegetation indices in winter. In spring, topographic variables had the most important role, and in summer, vegetation indices and edaphic variables were among the most important factors affecting plant diversity metrics [86]. Due to the mountainous nature of the studied area, it is likely that complex topographic features have shaped a variety of microclimates over a short distance [87], which could provide suitable microhabitats for a wide range of plant species holding different phenological and morphological characteristics [88]. Therefore, in this study, the topographic variables may have influenced plant diversity in summer and spring. Previous research confirmed the important role of topographical variables on plant diversity. Robinson et al. [89] stated that elevation is essential

for diversity estimations. Moreover, across the United States, Read et al. [90] have found that tree diversity was positively associated with elevation, slope, and aspect.

A higher importance of vegetation indices on plant diversity in winter can be due to the role of winter cold in limiting vegetation and subsequently plant diversity in the mountainous rangelands. In this regard, some vegetation indices, such as EVI and SATVI, showed these changes to be better than others. This may be due to a higher sensitivity of EVI to seasonal changes in canopy's biophysical attributes than other vegetation indices, which is in line with the previous study by Galvão et al. [91]. Moreover, SATVI has been demonstrated to capture temporal changes in grassland vegetation cover more efficiently than other vegetation indices because it relates with both live and senescent vegetation cover [39,92,93], potentially identifying changes related to vegetation. Interestingly, the variables characterizing the severe vegetation loss in July included high land surface temperature (LST), soil salinity, and deficit of rainfall, which are completely related to the condition of the arid regions in July.

Protecting biodiversity and ecosystem functioning is important for the delivery of basic services to human society. However, there are limitations in monitoring species diversity and figuring out the environmental factors that affect it in various geographic setups. The accelerating loss of biodiversity makes this problem even more important. It should be noted that ecosystem functions are rarely quantified, especially across large areas [94]. To solve this problem, satellite remote sensing, with relatively high temporal and spatial resolutions, offers global coverage and continuous measurements of plant diversity in space [95].

Among the limitations of this study were the scale of the study area and the relatively small number of samples, which were not especially well distributed throughout the region due to the severe topographic barriers in the study area. New opportunities to simultaneously measure plant structure and terrain morphology at fine spatial scales are presented by recent developments in airborne laser scanning (ALS). Therefore, it is necessary to address these issues in future studies by directly measuring environmental factors with grain sizes as small as tens of meters, which can reveal links between biodiversity and geodiversity at various scales.

Although the samples of this study were sufficient for conventional machine learning models, they were not optimal for deep learning. As a result, having more samples would enable the use of deep learning, which may prove more accurate. Therefore, these issues could be considered in future studies. Because grasslands located in different biomes clearly differ in the properties of plant species that inhabit them, the remotely sensed evaluation of their spectral diversity still needs to be biome-specific. It is also important to conduct similar studies on different scales to check whether the spectral diversity is scale-dependent or not.

5. Conclusions

This study provides insights into the usefulness of geodiversity and seasonal remotely sensed data in forecasting plant diversity patterns in dry rangelands. A non-linear model was used to predict vegetation cover, diversity, and richness. The link between plant diversity and reflectance is season-dependent, according to this study. The results complement the current knowledge, which is typically based on assessing the species diversity in the growing season. The accuracy of the models was enhanced by the use of satellite images taken during the peak of photosynthetic output and vegetation optimum (i.e., April). On the other hand, the use of satellite images taken in the middle of winter, when the leaf emergence for all deciduous species from the area is still incomplete, has led to a level of diversity, which is less than the actual level of diversity. Moreover, in vegetation diversity modeling, remotely sensed data might be more relevant than geodiversity data in winter and summer. Despite that, the geodiversity data had a greater contribution to the species diversity in the spring. Such evidence supports the integration of geodiversity and remotely sensed data for plant diversity monitoring and mapping across landscapes. The results

of such studies can be synthesized to provide documented information on plant diversity, which, in turn, will promote the conservation in rangeland ecosystems and will make it easier for ecologists to comprehend the temporal and spatial patterns of biodiversity.

Author Contributions: Conceptualization, S.R. and S.A.B.; formal analysis S.R.; investigation, S.R. and S.K.; methodology, S.R., A.A., S.M., V.N. and S.P.; software, S.R.; supervision, S.R. and S.A.B.; validation, S.R. and S.A.B.; visualization, S.R. and V.N.; writing, S.R.; writing—reviewing S.R., V.N. and S.A.B. All authors have read and agreed to the published version of the manuscript.

Funding: This work received no external funding.

Institutional Review Board Statement: Not applicable.

Informed Consent Statement: Not applicable.

Data Availability Statement: The data supporting the findings of this study are available from the first author (S.R.) upon reasonable request.

Acknowledgments: We thank to Hamed Gholizadeh for valuable and profound suggestions in the manuscript.

Conflicts of Interest: The authors declare no competing interest.

Appendix A

Table A1. Selected variables for modeling plant diversity in single-date and multi-seasonal models for each time milestone (February, April, and July).

Time Scale	Model	Variable
February	Geodiversity	TRI, TPI, MRVBF, MRRTF, MBI, Silt, ALT, pH, OM, EC, TWI, Rain, PRC, PLC, N, ASP
	Remotely sensed	NDWI, NDVIre2, NDre1, VSDI, SI, SATVI, MSI, HI, GNDVI, FeI, EVI, CRSI, CI, CalcI, CaI
	All data	VSDI, SI, SATVI, NDWI, NDVIre2, NDre1, MSI, HI, GNDVI, FeI, EVI, CRSI, CI, CalcI, CaI, TRI, TPI, MRVBF, MRRTF, MBI, Silt, ALT, pH, OM, LST, CN, EC, CLY, TWI, Rain, PRC, PLC, N, ASP
April	Geodiversity	ASP, ALT, PLC, PRC, Rain, Silt, TWI, EC, N OM, MBI, MRRTF, MRVBF, TPI, TRI, Lithology, Cly
	Remotely sensed	EVI, BI2, CalcI, CRSI, FeI, HI, NDVIre2, NMDI, SATVI, S3, TCIre1, LST, NDre2
	All data	NDVI, ASP, ALT, CN, EVI, EC, N, OM, PH, PLC, PRC, Rain, Silt, TWI, MBI, MRRTF, MRVBF, TPI, TRI, BI2, CalcI, CRSI, FeI, HI, NDVIre2, NMDI, SATVI, S3, TCIre1, Lithology, Clay, LST, NDre2
July	Geodiversity	ASP, ALT, Clay, EC, N, OM, pH, PLC, PRC, RN, SLP, SLT, TWI, NMDI, GRVI, Lithology, MBI, MRRTF, MRVBF, TPI
	Remotely sensed	EVI, FeI, GSI, HI, N, NDVI, LST, NDre2, S3, V, VDSI, NDVIre2, TCIre1, SATVI, CRSI
	All data	ASP, ALT, Clay, EC, EVI, FeI, GSI, HI, N, NDVI, OM, PH, LST, PLC, PRC, RN, SLP, SLT, TWI, NDre2, NMDI, GRVI, MSI, TVI, S3, V, VDSI, Lithology, NDVIre2, TCIre1, SATVI, MBI, MRRTF, MRVBF, TPI, CN, CRSI
Multi seasonal	Geodiversity	ASP, ALT, Cly, EC, N, OC, pH, PLC, PRC, Rain, SLP, Silt, TWI, MBI, MRRTF, MRVBF, TPI, TRI, CN
	Remotely sensed	BI2_April, CalcI_April, CaI_April, EVI_April, HI_April, LST_April, NDVI_April, NDre2_April, NMDI_April, NDWI_April, CRSI_April, MSAVI_April, SAVI_July, SMMI_July, TVI_July, V_July, VDSI_July, NDVIre1_July, TCIre1_July, SAVI_July, CRSI_July, LSTJ, LST_July, BI2_April, CalcI_April, FeI_April, GSI_April, NDVIre2_April, NMDI_April, SMMI_April, TCIre1_April, LST_April, BI_Feb, BI2_Feb, CaI_Feb, CalcI_Feb, CRSI_Feb, EVI_Feb, FeI_Feb, GNDVI_Feb, GSI_Feb, MSI_Feb, NDre2_Feb, NDVIre2_Feb, NDWI_Feb, SATVI_Feb, SMMI_Feb
	All data	ASP, ALT, BI, CaI, CalcI, CLY, EC, EVI, HI, LST, N, NDVI, OC, PH, PLC, PRC, Rain, SLP, Silt, TWI, NDre2_July, NMDI_July, NDWI_July, CRSI_July, LSWI_July, MSAVI_July, SAVI_July, SMMI_July, TVI_July, V_July, VDSI_July, Lithology, NDVIre2_July, TCIRE1_July, SATVI_July, MBI, MRRTF, MRVBF, TPI, TRI, CN, CRSI_July, LST_July, BI2_April, CalcI_April, FeI_April, GSI_April, NDVIre2_April, NMDI_April, SMMI_April, TCIre1_April, LST_April, BI_Feb, BI2_Feb, CaI_Feb, CalcI_Feb, CRSI_Feb, EVI_Feb, FeI_Feb, GNDVI_Feb, GSI_Feb, MSI_Feb, NDre2_Feb, NDVIre2_Feb, NDWI_Feb, SATVI_Feb, SMMI_Feb

References

1. Kissling, W.D.; Walls, R.; Bowser, A.; Jones, M.O.; Kattge, J.; Agosti, D.; Amengual, J.; Basset, A.; van Bodegom, P.M.; Cornelissen, J.H.C.; et al. Towards global data products of Essential Biodiversity Variables on species traits. *Nat. Ecol. Evol.* **2018**, *2*, 1531–1540. [CrossRef]
2. Rahmanian, S.; Hejda, M.; Ejtehadi, H.; Farzam, M.; Pyšek, P.; Memariani, F. Effects of livestock grazing on plant species diversity vary along a climatic gradient in northeastern Iran. *Appl. Veg. Sci.* **2020**, *23*, 551–561. [CrossRef]
3. Gotelli, N.J.; Colwell, R.K. Quantifying biodiversity: Procedures and pitfalls in the measurement and comparison of species richness. *Ecol. Lett.* **2001**, *4*, 379–391. [CrossRef]
4. Rahmanian, S.; Hejda, M.; Ejtehadi, H.; Farzam, M.; Memariani, F.; Pyšek, P. Effects of livestock grazing on soil, plant functional diversity, and ecological traits vary between regions with different climates in northeastern Iran. *Ecol. Evol.* **2019**, *9*, 8225–8237. [CrossRef] [PubMed]
5. He, K.S.; Bradley, B.A.; Cord, A.F.; Rocchini, D.; Tuanmu, M.-N.; Schmidtlein, S.; Turner, W.; Wegmann, M.; Pettorelli, N. Will remote sensing shape the next generation of species distribution models? *Remote Sens. Ecol. Conserv.* **2015**, *1*, 4–18. [CrossRef]
6. Rocchini, D.; Boyd, D.S.; Féret, J.-B.; Foody, G.M.; He, K.S.; Lausch, A.; Nagendra, H.; Wegmann, M.; Pettorelli, N. Satellite remote sensing to monitor species diversity: Potential and pitfalls. *Remote Sens. Ecol. Conserv.* **2016**, *2*, 25–36. [CrossRef]
7. Pettorelli, N.; Laurance, W.F.; O'Brien, T.G.; Wegmann, M.; Nagendra, H.; Turner, W. Satellite remote sensing for applied ecologists: Opportg for applied eco ¨

26. Silveira, E.M.; Radeloff, V.C.; Martinuzzi, S.; Pastur, G.J.M.; Rivera, L.O.; Politi, N.; Lizarraga, L.; Farwell, L.S.; Elsen, P.R.; Pidgeon, A.M. Spatio-temporal remotely sensed indices identify hotspots of biodiversity conservation concern. *Remote Sens. Environ.* **2021**, *258*, 112368. [CrossRef]
27. Reddy, C.S. Remote sensing of biodiversity: What to measure and monitor from space to species? *Biodivers. Conserv.* **2021**, *30*, 2617–2631. [CrossRef]
28. Oldeland, J.; Wesuls, D.; Rocchini, D.; Schmidt, M.; Jürgens, N. Does using species abundance data improve estimates of species diversity from remotely sensed spectral heterogeneity? *Ecol. Indic.* **2010**, *10*, 390–396. [CrossRef]
29. Féret, J.B.; Asner, G.P. Mapping tropical forest canopy diversity using high-fidelity imaging spectroscopy. *Ecol. Appl.* **2014**, *24*, 1289–1296. [CrossRef]
30. Schäfer, E.; Heiskanen, J.; Heikinheimo, V.; Pellikka, P. Mapping tree species diversity of a tropical montane forest by unsupervised clustering of airborne imaging spectroscopy data. *Ecol. Indic.* **2016**, *64*, 49–58. [CrossRef]
31. Wang, R.; Gamon, J.A.; Schweiger, A.K.; Cavender-Bares, J.; Townsend, P.A.; Zygielbaum, A.I.; Kothari, S. Influence of species richness, evenness, and composition on optical diversity: A simulation study. *Remote Sens. Environ.* **2018**, *211*, 218–228. [CrossRef]
32. Fuhlendorf, S.D.; Fynn, R.W.; McGranahan, D.A.; Twidwell, D. Heterogeneity as the basis for rangeland management. In *Rangeland Systems*; Briske, D.D., Ed.; Springer: Cham, Switzerland, 2017; pp. 169–196.
33. Karami, S.; Khosravi, A.R. A Floristic Study of Kuh-e Dakal in Mamasani County, Fars Province. *J. Taxon. Biosyst.* **2019**, *11*, 1–12.
34. Scudiero, E.; Skaggs, T.H.; Corwin, D.L. Regional-scale soil salinity assessment using Landsat ETM+ canopy reflectance. *Remote Sens. Environ.* **2015**, *169*, 335–343. [CrossRef]
35. Chen, Y.; Qiu, Y.; Zhang, Z.; Zhang, J.; Chen, C.; Han, J.; Liu, D. Estimating salt content of vegetated soil at different depths with Sentinel-2 data. *PeerJ* **2020**, *8*, e10585. [CrossRef]
36. Gitelson, A.A.; Kaufman, Y.J.; Merzlyak, M.N. Use of a green channel in remote sensing of global vegetation from EOS-MODIS. *Remote Sens. Environ.* **1996**, *58*, 289–298. [CrossRef]
37. Rouse, J.W., Jr.; Haas, R.H.; Deering, D.W.; Schell, J.A.; Harlan, J.C. *Monitoring the Vernal Advancement and Retrogradation (Green Wave Effect) of Natural Vegetation*; NASA/GSFCT Type III Final Report; No. E75-10354; NASA: Greenbelt, MD, USA, 1974.
38. Khalid, H.W.; Khalil, R.M.Z.; Qureshi, M.A. Evaluating spectral indices for water bodies extraction in western Tibetan Plateau. *Egypt. J. Remote Sens. Space Sci.* **2021**, *24*, 619–634.
39. Marsett, R.C.; Qi, J.; Heilman, P.; Biedenbender, S.H.; Watson, M.C.; Amer, S.; Weltz, M.; Goodrich, D.; Marsett, R. Remote sensing for grassland management in the arid southwest. *Rangel. Ecol. Manag.* **2006**, *59*, 530–540. [CrossRef]
40. Qi, J.; Chehbouni, A.; Huete, A.R.; Kerr, Y.H.; Sorooshian, S. A modified soil adjusted vegetation index. *Remote Sens. Environ.* **1994**, *48*, 119–126. [CrossRef]
41. Yue, J.; Tian, J.; Tian, Q.; Xu, K.; Xu, N. Development of soil moisture indices from differences in water absorption between shortwave-infrared bands. *ISPRS J. Photogramm. Remote Sens.* **2019**, *154*, 216–230. [CrossRef]
42. Jordan, C.F. Derivation of leaf-area index from quality of light on the forest floor. *Ecology* **1969**, *50*, 663–666. [CrossRef]
43. Raya, S.S.; Singhb, J.P.; Dasa, G.; Panigrahyb, S. Use of high resolution remote sensing data for generating site-specific soil mangement plan. *Red* **2004**, *550*, 727.
44. Amen, A.; Blaszczynski, J. *Integrated Landscape Analysis*; US Department of the Interior, Bureau of Land Management, National Science and Technology Center: Denver, CO, USA, 2001.
45. Nield, S.J.; Boettinger, J.L.; Ramsey, R.D. Digitally mapping gypsic and natric soil areas using Landsat ETM data. *Soil Sci. Soc. Am. J.* **2007**, *71*, 245–252. [CrossRef]
46. Xiao, J.; Shen, Y.; Tateishi, R.; Bayaer, W. Development of topsoil grain size index for monitoring desertification in arid land using remote sensing. *Int. J. Remote Sens.* **2006**, *27*, 2411–2422. [CrossRef]
47. Triki Fourati, H.; Bouaziz, M.; Benzina, M.; Bouaziz, S. Modeling of soil salinity within a semi-arid region using spectral analysis. *Arab. J. Geosci.* **2015**, *8*, 11175–11182. [CrossRef]
48. Rock, B.N.; Hoshizaki, T.; Miller, J.R. Comparison of in situ and airborne spectral measurements of the blue shift associated with forest decline. *Remote Sens. Environ.* **1988**, *24*, 109–127. [CrossRef]
49. Allbed, A.; Kumar, L.; Aldakheel, Y.Y. Assessing soil salinity using soil salinity and vegetation indices derived from IKONOS high-spatial resolution imageries: Applications in a date palm dominated region. *Geoderma* **2014**, *230*, 1–8. [CrossRef]
50. Escadafal, R.; Girard, M.C.; Courault, D. Munsell soil color and soil reflectance in the visible spectral bands of Landsat MSS and TM data. *Remote Sens. Environ.* **1989**, *27*, 37–46. [CrossRef]
51. Williams, D. *Landsat-7 Science Data User's Handbook*; National Aeronautics and Space Administration: Greenbelt, MD, USA, 2009; p. 186.
52. Wilson, J.P.; Gallant, J.C. Digital Terrain Analysis. In *Terrain Analysis: Principles and Applications*; Wilson, J.P., Gallant, J.C., Eds.; John Wiley Sons: New York, NY, USA, 2000; pp. 1–27.
53. Gallant, J.C.; Dowling, T.I. A multi resolution index of valley bottom flatness for mapping depositional areas. *Water Resour. Res.* **2003**, *39*, 1347–1360. [CrossRef]
54. Moore, I.D.; Gessler, P.; Nielsen, G.; Peterson, G. Soil attribute prediction using terrain analysis. *Soil Sci. Soc. Am. J.* **1993**, *57*, 443–452. [CrossRef]
55. Weiss, J.B.; Suyama, K.L.; Lee, H.H.; Scott, M.P. Jelly belly: A Drosophila LDL receptor repeat-containing signal required for mesoderm migration and differentiation. *Cell* **2001**, *107*, 387–398. [CrossRef]

56. Riley, S.J.; DeGloria, S.D.; Elliot, R. Index that quantifies topographic heterogeneity. *Intermt. J. Sci.* **1999**, *5*, 23–27.
57. Lu, G.Y.; Wong, D.W. An adaptive inverse-distance weighting spatial interpolation technique. *Comput. Geosci.* **2008**, *34*, 1044–1055. [CrossRef]
58. Tuanmu, M.N.; Jetz, W. A global, remote sensing-based characterization of terrestrial habitat heterogeneity for biodiversity and ecosystem modelling. *Glob. Ecol. Biogeogr.* **2015**, *24*, 1329–1339. [CrossRef]
59. Kim, J.H. Multicollinearity and misleading statistical results. *Korean J. Anesthesiol.* **2019**, *72*, 558–569. [CrossRef] [PubMed]
60. Pielou, E.C. Shannon's formula as a measure of specific diversity: Its use and misuse. *Am. Nat.* **1966**, *100*, 463–465. [CrossRef]
61. Simpson, E.H. Measurement of diversity. *Nature* **1949**, *163*, 688. [CrossRef]
62. Hooper, D.U.; Solan, M.; Symstad, A.; Diaz, S.; Gessner, M.O.; Buchmann, N.; Degrange, V.; Grime, P.; Hulot, F.; Mermillod-Blondin, F.; et al. Species diversity, functional diversity and ecosystem functioning. In *Biodiversity and Ecosystem Functioning: Synthesis and Perspectives*; Oxford University Press: Oxford, UK, 2002; pp. 195–208.
63. Pearson, K.X. Contributions to the mathematical theory of evolution.—II. Skew variation in homogeneous material. *Philos. Trans. R. Soc. Lond. A* **1895**, *186*, 343–414.
64. Bowman, D.T. Contemporary issues. *J. Cotton Sci.* **2001**, *5*, 137–141.
65. Breiman, L. Random forests. *Mach. Learn.* **2001**, *45*, 5–32. [CrossRef]
66. Rahmanian, S.; Pourghasemi, H.R.; Pouyan, S.; Karami, S. Habitat potential modelling and mapping of Teucrium polium using machine learning techniques. *Environmental Monitoring and Assessment* **2021**, *193*, 1–21. [CrossRef]
67. Nasiri, V.; Sadeghi, S.M.M.; Moradi, F.; Afshari, S.; Deljouei, A.; Griess, V.C.; Maftei, C.; Borz, S.A. The Influence of Data Density and Integration on Forest Canopy Cover Mapping Using Sentinel-1 and Sentinel-2 Time Series in Mediterranean Oak Forests. *ISPRS Int. J. Geo-Inf.* **2022**, *11*, 423. [CrossRef]
68. Liaw, A.; Wiener, M. Classification and regression by randomForest. *R News* **2002**, *2*, 18–22.
69. Kuhn, M. A Short Introduction to the caret Package. *R Found Stat Comput* **2015**, *1*, 1–10.
70. Wei, P.; Lu, Z.; Song, J. Variable importance analysis: A comprehensive review. *Reliab. Eng. Syst. Saf.* **2015**, *142*, 399–432. [CrossRef]
71. Uyanık, T.; Karatuğ, Ç.; Arslanoğlu, Y. Machine learning approach to ship fuel consumption: A case of container vessel. *Transp. Res. Part D: Transp. Environ.* **2020**, *84*, 102389. [CrossRef]
72. Wang, W.; Lu, Y. Analysis of the mean absolute error (MAE) and the root mean square error (RMSE) in assessing rounding model. *IOP Conf. Ser. Mater. Sci. Eng.* **2018**, *324*, 012049. [CrossRef]
73. Chrysafis, I.; Mallinis, G.; Tsakiri, M.; Patias, P. Evaluation of single-date and multi-seasonal spatial and spectral information of Sentinel-2 imagery to assess growing stock volume of a Mediterranean forest. *Int. J. Appl. Earth Obs. Geoinf.* **2019**, *77*, 1–14. [CrossRef]
74. Chrysafis, I.; Korakis, G.; Kyriazopoulos, A.P.; Mallinis, G. Predicting Tree Species Diversity Using Geodiversity and Sentinel-2 Multi-Seasonal Spectral Information. *Sustainability* **2020**, *12*, 9250. [CrossRef]
75. Senf, C.; Leitão, P.J.; Pflugmacher, D.; van der Linden, S.; Hostert, P. Mapping land cover in complex Mediterranean landscapes using Landsat: Improved classification accuracies from integrating multi-seasonal and synthetic imagery. *Remote Sens. Environ.* **2015**, *156*, 527–536. [CrossRef]
76. Ehrlinger, J. ggRandomForests: Exploring random forest survival. *arXiv* **2016**, arXiv:1612.08974.
77. Wolter, P.T.; Mladenoff, D.J.; Host, G.E.; Crow, T.R. Using multi-temporal landsat imagery. *Photogramm. Eng. Remote Sens* **1995**, *61*, 1129–1143.
78. Hill, R.A.; Wilson, A.K.; George, M.; Hinsley, S.A. Mapping tree species in temperate deciduous woodland using time-series multi-spectral data. *Appl. Veg. Sci.* **2010**, *13*, 86–99. [CrossRef]
79. Kampouri, M.; Kolokoussis, P.; Argialas, D.; Karathanassi, V. Mapping of Forest Tree Distribution and Estimation of Forest Biodiversity using Sentinel-2 Imagery in the University Research Forest Taxiarchis in Chalkidiki, Greece. *Geocarto Int.* **2019**, *34*, 1273–1285. [CrossRef]
80. Torresani, M.; Rocchini, D.; Sonnenschein, R.; Zebisch, M.; Marcantonio, M.; Ricotta, C.; Tonon, G. Estimating tree species diversity from space in an alpine conifer forest: The Rao's Q diversity index meets the spectral variation hypothesis. *Ecol. Inform.* **2019**, *52*, 26–34. [CrossRef]
81. Arekhi, M.; Yılmaz, O.Y.; Yılmaz, H.; Akyüz, Y.F. Can tree species diversity be assessed with Landsat data in a temperate forest? *Environ. Monit. Assess.* **2017**, *189*, 586. [CrossRef]
82. Hernández-Stefanoni, J.L.; Gallardo-Cruz, J.A.; Meave, J.A.; Rocchini, D.; Bello-Pineda, J.; López-Martínez, J.O. Modeling α-and β-diversity in a tropical forest from remotely sensed and spatial data. *Int. J. Appl. Earth Obs. Geoinf.* **2012**, *19*, 359–368. [CrossRef]
83. Hurlbert, A.H.; Haskell, J.P. The effect of energy and seasonality on avian species richness and community composition. *Am. Nat.* **2003**, *161*, 83–97. [CrossRef] [PubMed]
84. Feeley, K.J.; Gillespie, T.W.; Terborgh, J.W. The Utility of Spectral Indices from Landsat ETM+ for Measuring the Structure and Composition of Tropical Dry Forests 1. *Biotropica J. Biol. Conserv.* **2005**, *37*, 508–519.
85. Lassau, S.A.; Cassis, G.; Flemons, P.K.; Wilkie, L.; Hochuli, D.F. Using high-resolution multi-spectral imagery to estimate habitat complexity in open-canopy forests: Can we predict ant community patterns? *Ecography* **2005**, *28*, 495–504. [CrossRef]

86. Prăvălie, R.; Sîrodoev, I.; Nita, I.A.; Patriche, C.; Dumitraşcu, M.; Roşca, B.; Tişcovschi, A.; Bandoc, G.; Săvulescu, I.; Mănoiu, V.; et al. NDVI-based ecological dynamics of forest vegetation and its relationship to climate change in Romania during 1987–2018. *Ecol. Indic.* **2022**, *136*, 108629. [CrossRef]
87. Scherrer, D.; Körner, C. Topographically controlled thermal-habitat differentiation buffers alpine plant diversity against climate warming. *J. Biogeogr.* **2011**, *38*, 406–416. [CrossRef]
88. Opedal, Ø.H.; Armbruster, W.S.; Graae, B.J. Linking small-scale topography with microclimate, plant species diversity and intra-specific trait variation in an alpine landscape. *Plant Ecol. Divers.* **2015**, *8*, 305–315. [CrossRef]
89. Robinson, C.; Saatchi, S.; Clark, D.; Astaiza, J.H.; Hubel, A.F.; Gillespie, T.W. Topography and three-dimensional structure can estimate tree diversity along a tropical elevational gradient in Costa Rica. *Remote Sens.* **2018**, *10*, 629. [CrossRef]
90. Read, Q.D.; Zarnetske, P.L.; Record, S.; Dahlin, K.M.; Costanza, J.K.; Finley, A.O.; Gaddis, K.D.; Grady, J.M.; Hobi, M.L.; Latimer, A.M.; et al. Beyond counts and averages: Relating geodiversity to dimensions of biodiversity. *Glob. Ecol. Biogeogr.* **2020**, *29*, 696–710. [CrossRef]
91. Galvão, L.S.; Breunig, F.M.; Teles, T.S.; Gaida, W.; Balbinot, R. Investigation of terrain illumination effects on vegetation indices and VI-derived phenological metrics in subtropical deciduous forests. *GIScience Remote Sens.* **2016**, *53*, 360–381. [CrossRef]
92. Goirán, S.B.; Aranibar, J.N.; Gomez, M.L. Heterogeneous spatial distribution of traditional livestock settlements and their effects on vegetation cover in arid groundwater coupled ecosystems in the Monte Desert (Argentina). *J. Arid. Environ.* **2012**, *87*, 188–197. [CrossRef]
93. Hagen, M.; Kissling, W.D.; Rasmussen, C.; De Aguiar, M.A.M.; Brown, L.E.; Carstensen, D.W.; Alves-Dos-Santos, I.; Dupont, Y.L.; Edwards, F.K.; Genini, J.; et al. Biodiversity, species interactions and ecological networks in a fragmented world. In *Advances in Ecological Research*; Academic Press: Cambridge, MA, USA, 2012; Volume 46, pp. 89–210.
94. Pettorelli, N.; Bühne, H.S.T.; Tulloch, A.; Dubois, G.; Macinnis-Ng, C.; Queirós, A.M.; Keith, D.A.; Wegmann, M.; Schrodt, F.; Stellmes, M.; et al. Satellite remote sensing of ecosystem functions: Opportunities, challenges and way forward. *Remote Sens. Ecol. Conserv.* **2018**, *4*, 71–93. [CrossRef]
95. Turner, W.; Spector, S.; Gardiner, N.; Fladeland, M.; Sterling, E.; Steininger, M. Remote sensing for biodiversity science and conservation. *Trends Ecol. Evol.* **2003**, *18*, 306–314. [CrossRef]